TRANSIENT BEAM LOADING EFFECTS IN RF SYSTEMS IN JLEIC*

Haipeng. Wang[#], Jiquan Guo, Robert A. Rimmer and Shaoheng Wang
Thomas Jefferson Lab, Newport News, VA 23606, USA

Abstract

The pulsed electron bunch trains generated from the Continuous Electron Beam Accelerator Facility (CEBAF) linac to inject into the proposed Jefferson Lab Electron Ion Collider (JLEIC) e-ring will produce transient beam loading effects in the Superconducting Radio Frequency (SRF) systems that, if not mitigated, could cause unacceptably large beam energy deviation in the injection capture, or exceed the energy acceptance of CEBAF's recirculating arcs. In the electron storage ring, the beam abort or ion clearing gaps or uneven bucket filling can cause large beam phase transients in the (S)RF cavity control systems and even beam loss due to Robinson instability. We have first analysed the beam stability criteria in steady state and estimated the transient effect in Feedforward and Feedback RF controls. Initial analytical models for these effects are shown for the design of the JLEIC e-ring from 3GeV to 12GeV.

INTRODUCTION

The conceptual design of a staged JLEIC was updated in 2015 [1]. Its Figure-8 layout using the CEBAF as the electron injector and the RF systems using both normal conducting (NC) and superconducting (SC) technology for electron and ions acceleration are shown in Figure 1. The technical challenge for the CEBAF machine, which is a CW SC RF machine operated at 1497MHz, will be in a pulse mode operation in order to inject electron bunches into the 476.3MHz electron ring, which is based PEP-II components. The time structure of bunch trains from the injector gun to CEBAF (using the North Linac as an example), and then filling in to the electron ring has been updated since last published [2] as shown in Figure 2. Due to the requirement that electron polarization in the Figure-8 has to be one half of the ring up and the other half down with two gaps between them the CABAF has to be operated in a pulsed beam mode with alternative polarizations. The horizontal injection scheme needs to leave enough damping time (6-350ms) between injection cycles. The bunch frequency within the train (3.23μs) has to be 68.05MHz.

RF TRANSIENT IN CEBAF LINAC

The transient effect on the CEBAF SRF system could happen between the bunch trains (0.97μs), since the CEBAF circulation time is 4.2μs and bunch train length is 3.23μs and between the polarization switching time (6-350ms, also allowing for injection damping). A general RF cavity voltage V_c with time varying beam loading and klystron incident power P_{in} with no phase change on resonance can be expressed as (1):

$$V_c(t) = e^{-\frac{t-t_0}{T_f}}\left(V_{c0} + \frac{1}{T_f}\int_{t_0}^{t} e^{\frac{t-t_0}{T_f}}\left(\frac{2Q_L}{Q_e}\sqrt{\frac{R}{Q}Q_e P_{in}(t)} - \frac{R}{Q}Q_L I_b(t)\right)dt\right) \quad (1)$$

For a periodic pulsed beam current,

$$I_b = \begin{cases} I_b, & nT_0 < t < nT_0 + T_p \\ 0, & nT_0 + T_p < t < (n+1)T_0 \end{cases} \quad (2)$$

If we have a fixed P_{in}:

$$V_c(t) = \frac{2Q_L}{Q_e}\sqrt{P_{in}\frac{R}{Q}Q_e} - e^{\frac{nT_0+T_p-T_0-t}{T_f}}$$

$$- \begin{cases} V_I\left(1 - e^{\frac{-T_p}{T_f}}\right), & nT_0 < t < nT_0 + T_p \\ V_I e^{\frac{T_0-t}{T_f}}\left(e^{\frac{T_p}{T_f}} - 1\right), & nT_0 + T_p < t < (n+1)T_0 \end{cases} \quad (3)$$

Here $T_f = \frac{Q_L}{\omega}$, $V_I = \frac{R}{Q}Q_L I_b$, T_0 is bunch train period, T_p is bunch train pulse time, $\frac{Q_L}{Q_e} = \frac{1+\beta}{\beta}$ and n is the bunch number.
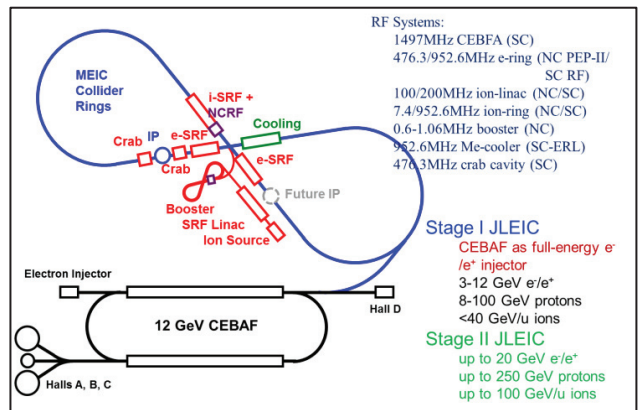

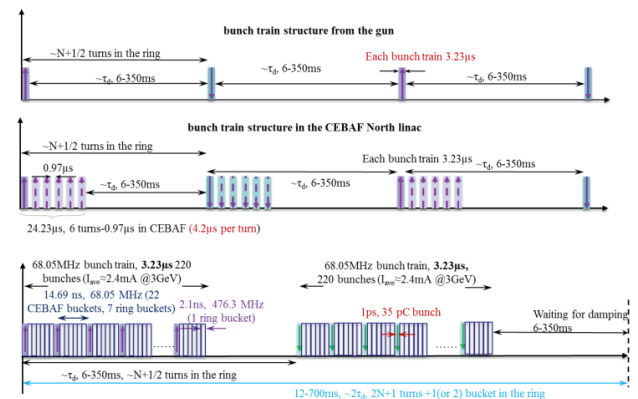Figure 1: Layout of conceptual design of staged JLEIC with NC and SC RF systems.

Figure 2: Time structure of electron bunch trains from injector gun to CEBAF and then to Figure-8 electron ring.

Assuming using only the new digital Low Level RF (LLRF) control for the feedback, the relative energy droop calculated by equations (1-3) for the beam energy >6GeV seem to be less than 0.2% which is within a typical circulating arc acceptance. For lower beam energy operation, a feedforward (FF) control to the klystron power has been proposed. This adaptive feedforward function has been designed as a build-in function in the 12 GeV upgrade digital LLRF controller. An ideal pulse drive signal synchronized with the beam bunch train is:

$$\frac{2Q_L}{Q_e}\sqrt{\frac{R}{Q}Q_e P_{in}(t)} = V_c + \frac{R}{Q}Q_L I_b(t)\cos\phi \qquad (4)$$

Figure 3 illustrates that the voltage droop could be 0.38% without the FF but drops to 0.015% with the FF. Such a small droop is due to the rise and fall time of the klystron from 1.44kW during the gaps to 5.85kW during the bunch train, which also leaves enough head room for the 13kW klystron to control cavity microphonics.
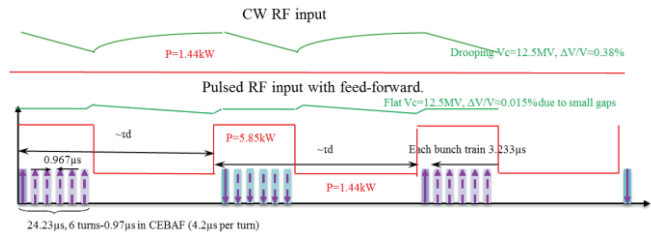

Figure 3: Typical C100 cavity voltage pulse shapes without FF (upper green trace) and with FF (lower green trace) at 12.5MV with a 0.4mA peak current.

Table 1 lists the voltage droop with the FF control for three types of SRF cavities at CEBAF to operate at 3GeV. To be able to achieve $\Delta P/P < 0.2\%$, lowering the external Q_e by stub tuners and lowering bunch charge for a longer injection time have to be considered.

Table 1: Calculated Cavity Voltage Droops in CEBAF with FF and the Injection Time to JLEIC at Low Energies

Cavity type	Desired Q_e	Vc (MV)	Klystron power (kW)	Energy (GeV)	Ib_{ext} (μA)	Ib_{ext} (μA) Current CEBAF CW	Q/bunch, 68MHz (pC)	$2\tau d$ (ms)	$\Delta Vc/Vc$	$\Delta p/p$	JLEIC injection time (minutes)
C100	1×10^7	3	4.9			~100 (Due to BBU)	22	750	0.14%		
C50	6.6×10^6	1	1.7	3	1500				0.25%	0.2%	~25
C20	6.6×10^6	1	1.7						0.25%		
C100	3.3×10^6	3	6						0.24%		
C50	3.3×10^6	1	2.4	3	2400	~100	35.2	750	0.40%	0.33%	~16
C20	3.3×10^6	1	2.4						0.40%		
C100	1×10^7	6	5.7						0.06%		
C50	6.6×10^6	2	1.9	6	1200	~170	17.6	71	0.10%	0.08%	~3
C20	6.6×10^6	2	1.9						0.10%		

RF TRANSIENT IN ELECTRON RING

Most recent studies on the transient beam loading to the electron storage ring RF system rely on the beam dynamic tracking simulations, particularly for the beam injection, top-off and uneven-filling time structure as well as bunch lengthening [3-5]. However when the additional RF feedback or extra cavity system is involved, their circuit models and the transient envelope (state-space) equation in Simulink modelling can also be [5-6]. Such a simulation method for a conceptual design with a large parameter range is not straightforward, particularly when the Robinson [7] or Pedersen [8-9] stability criteria is invalid. An analytical approach to assess the Robinson stability with direct feedback (DFB) model was derived by Wang [10] using current vectors as the circuit model as shown in Figure 4, An exact solution is also given by Heifets using voltage vectors instead in the circuit model [11]. Using the analytical model, a MathCAD program has been developed. Since the beam transient effect is more severe at low energy, we studied an example of 3GeV, 1.994A beam current on a 952.6MHz SC RF cavity for the JLEIC design.
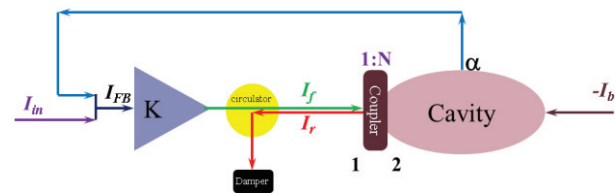

Figure 4: RF cavity direct feedback model with beam loading, where the loop gain $A = \alpha K$.

In this way the transient control with and without a DFB can be compared. Figure 5 shows the Robinson stability diagram without feedback and without feedback and with feedback for two different loop delays. For the shorter loop delay the working point is more stable, but for the longer example it is unstable, and the gain would have to be reduced. Figure 6 shows the real part of the cavity impedance as a function of gain and loop delay. Figure 7 shows the constant klystron forward power contour lines P_{for} on the Robinson diagram [12]. The minimum klystron power follows the loading line through the working point. Where the load line intercepts the stability boundary determines the maximum stable beam current and the minimum klystron power needed to support that current. Additional klystron power headroom is needed when a beam transient exists. Such a transient effect can be seen

more directly on the plot of beam loading ratio Y verses klystron loading angle like Pedersen has used [8-9], where the cavity voltage V_{cell1}, beam current I_b, DFB loop gain A and group delay τ_d and cavity detune angle ψ_2 are all constants. The maximum synchronous phase transient
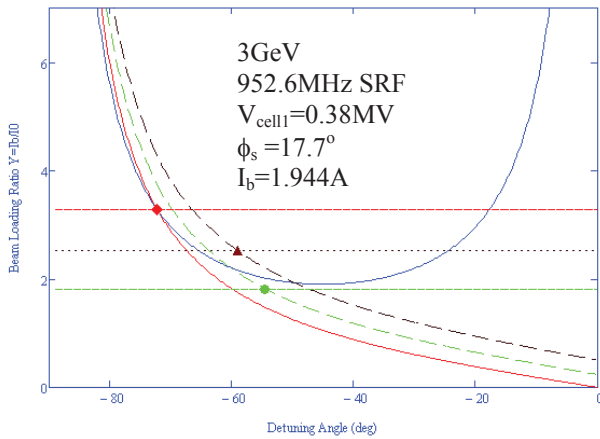

Figure 5: Robinson stability diagram: below the blue line and between the -90<detuning angle<0 range is the stable area for above transition operation. Red curved line is a specific loading angle through the working point which is the interception point (red diamond symbol) with Y loading line (red dash-straight) in open loop. With a DFB of gain A=1, and a delay τ_d=0.4μs the working point is more stable (green dot), however a longer group delay τ_d=0.8μs could make the working point unstable (black triangle symbol).
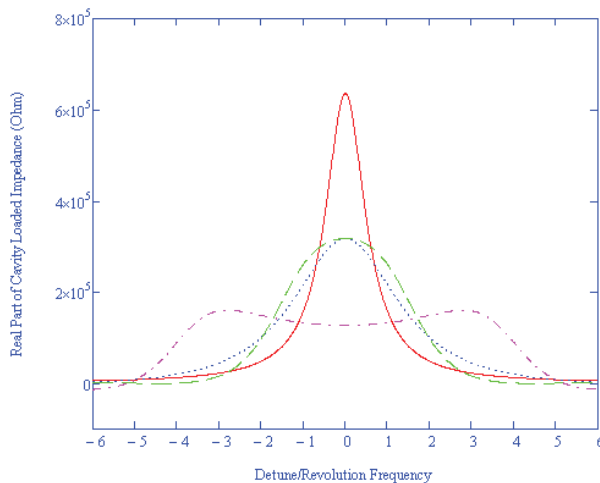

Figure 6: Real part of cavity impedance: red solid, A=0; blue dot-line, A=1, τ_d=0.4μs; green dash-line, A=1, τ_d=0.8μs; magenta dot-dash-line, A=4, τ_d=0.4μs. All input parameters are same as in Figure 5.

should be as same as the loading angle change [13] which is controlled by the DFB. Its steady state can be only maintained within the headroom of klystron power and under the stable Robinson boundary as shown in Figure 8. Such a transient limit can only tolerate the beam gap of 32.3m or only 1.5% of ring's circumference which the

maximum transient phase calculation formula can be found in [14]. In addition, other stability criteria checks from ref. [15] are also studied and satisfied.
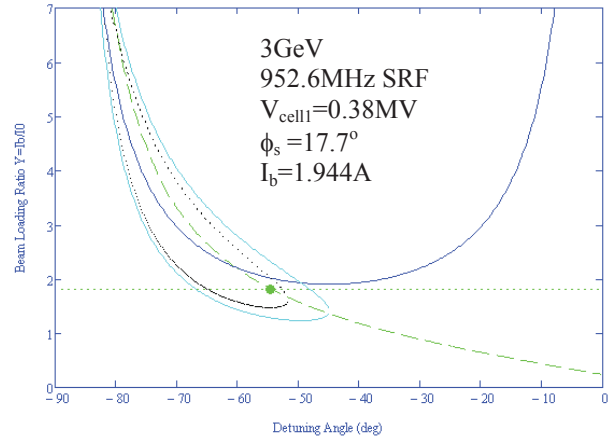

Figure 7: Robinson diagram showing working point with A=1, τ_d=0.4μs, and contours for P_{for}=260kW (black dot-line) and P_{for}=280kW (cyan solid-line).
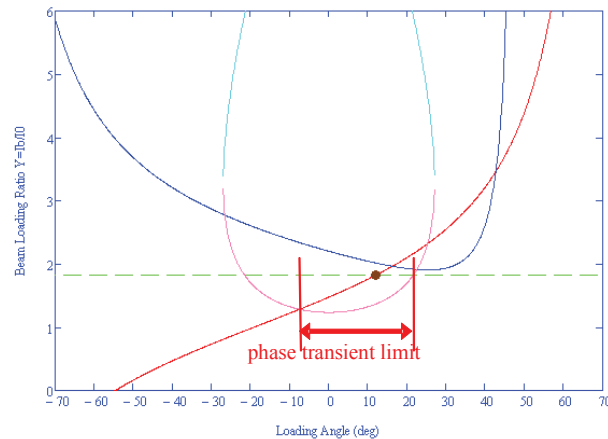

Figure 8: Pedersen diagram showing the estimated beam synchronous phase transient limit. Klystron power contour line (magenta) is for 280kW. Other parameters are same as in Figure 7.

For a cross-check with experimental data, a recent result of BEPC-II running with the highest luminosity was obtained. The calculation of this model indicates that the beam phase transient is actually limited by the Robinson boundary in only about 0.8° range. The actual beam gap (and bunch spaing) in the final machine setup is indeed less than this (0.36°) which validates this model.

ACKNOWLEDGEMENT

REFERENCES

[1] F. Lin etc., Proceedings of IPAC 2015, TUYB3

[2] J. Guo etc., Proceedings of IPAC 2015, TUYTY083

[3] J. M. Byrd, etc., PRST-AB 5, 092001 (2002)

[4] M. Borland, T. Berenc etc., Proceedings of IPAC 2015, MOPMA006 and MOPMA007

[5] A. Neumann etc., Proceedings of IPAC 2015, MOPHA010

[6] T. Kobayashi, presentation for SuperKEKB review, April 24, 2015

[7] K.W. Robinson, CEAL-1010, MIT and Harvard University, Cambridge Electron Accelerator, February 1964

[8] F. Pedersen, IEEE Trans. Nuclear Science, Vol. NS-22, No. 3, June 1975, Proceedings of PAC 1975

[9] F. Pedersen, IEEE Trans. on Nuclear Science, Vol. NS-32, No. 5, Oct. 1985.

[10] Shaoheng Wang, Direct Feedback, unpublished, April, 2015

[11] S. Heifets and D. Teytelman, PRST-AB 10, 012804 (2007)

[12] H. Wang, S. Wang, Derivation of the constant power contour lines in Robinson stability diagram, Note rewritten on January 13, 2016

[13] P. B. Wilson, SLAC-PUB-6062, March 1993

[14] D. Boussard, Proceeding of PAC 1991, p2447

[15] S. Koscielniak, Particle Accelerators, ©1999 OPA N.V. Vol. 62, pp. 179-214